J|A|C|S COMMUNICATIONS

Published on Web 11/23/2009

Spectrally Tunable Leakage-Free Gold Nanocontainers

Yongdong Jin and Xiaohu Gao*

Department of Bioengineering, University of Washington, William H. Foege Building N530M, Seattle, Washington 98195

Received September 19, 2009; E-mail: xgao@u.washington.edu

Recently there has been a burst of activity on the design and engineering of plasmonically responsive nanostructures for remotely controlled delivery of therapeutics.[1−6] These techniques generally rely on the unique photothermal conversion property of metallic nanostructures when irradiated at the nanostructures' surface plasmon resonance (SPR), which can be tuned to the near-infrared (NIR) region for deep tissue penetration. Two general formats exist for loading of cargo molecules. In the first approach, molecules of interest including both small organic molecules and oligonucleotides are attached to the surface of gold nanorods (gNRs) or nanoprisms and are released upon NIR illumination.[2−4,7,8] In the second approach, gold nanoparticles are combined with liposomes (e.g., by adsorbing on, forming large aggregates with, or embedding inside liposomes) loaded with cargo molecules. Similar to the first approach, upon NIR light absorption, gold nanoparticles destabilize liposomes leading to content release.[5,6,9]

Despite these recent advances, a key limitation shared by the existing technologies is that leakage or degradation of cargo molecules is inevitable. For example, small-molecule drugs immobilized on nanoparticle surfaces can slowly diffuse away,[10] whereas surface bound oligonucleotides are still accessible to enzymes.[11] Similarly, trapping drugs inside liposomes or micelles do not solve the problem either, because it is widely known that liposomes and micelles are metastable and can rupture in blood circulation before reaching targeted cells.[12] Recent work by Cheng and co-workers shows that cargo molecules loaded in micelles are significantly released *in vivo* within 15 min post intravenous injection.[13,14] A dual-color Förster resonance energy transfer assay allows monitoring of the release process in real time, and the results suggest the urgent need for improved drug carriers. Thus, the ability to create nanocontainers that are *simultaneously* being leakage-free in circulation (or under storage) and able to release cargo in an 'on-demand' fashion is of considerable interest. Here, we report a new generation of nanocontainers that are leakage-free, spectrally programmable, and capable of monitoring drug release.

As shown in Figure 1a, cargo loaded liposomes are encapsulated with a thin shell of gold, which is biocompatible but nonbiodegradable. The spatially confined gold shell growth is directed by a layer of poly-L-histidine (PLH) on the liposome surface, which is capable of chelating metal ions.[15] In contrast to liposome−gold nanoparticle clusters,[5,6,9] the integrity of our nanocontainer is determined by the gold shell instead of the original liposome, thus rendering the nanocontainer stable and the embedded cargo unavailable at the ambient temperature. The nanocontainers' SPR spectra are tunable by varying the overall particle size and shell thickness. It is well established that photothermal heating based on gold nanostructures under pulsed laser irradiation can dramatically increase *local* temperature or even melt nanoparticles,[16,17] resulting in content release. This design has a number of important features. For example, drug release can be spatially confined to targeted sites and help reduce toxicity to other organs. In addition, the release profile can be precisely controlled for optimal dosage using laser illumination at various powers.

Figure 1b−d show the transmission electron microscopy (TEM) images of nanocontainers of three different sizes, which are determined by the liposomal scaffold. These as-synthesized hollow gold spheres are well-dispersed and uniform with diameters of 10 ± 3, 20 ± 5, and 70 ± 10 nm, respectively (measured from >100 nanoparticles for each sample). The shell thickness is adjustable by changing the amount of gold ions during gold shell formation and is ∼2 to 5 nm in the current study. The hollow spheres and the shell thickness are further characterized by high-resolution TEM (HRTEM) for the 10 and 20 nm samples. A zoomed-in view in the inset images clearly shows the metal shell. We were not able to perform HRTEM on the 70 nm sample because they were unstable under electron beam irradiation. Particle melting and collapse were observed within a few seconds (the smaller nanocontainers can tolerate electron irradiation slightly longer for HRTEM). Figure 1e shows the corresponding extinction spectra of the three nanocontainers. The extinction bands of the 10, 20, and 70 nm shells are centered at ∼ 600, 690, and 750 nm, respectively, with the latter two in the NIR spectral window.

To probe the nanocontainer stability and its cargo release capability, an organic dye (carboxyfluorescein, or FAM) labeled liposome was used as a model system. Figure 2a−d show the imaging and spectroscopy measurements of gold nanocontainers prepared from the FAM loaded liposomes. The nanocontainers are 18 ± 5 nm in diameter with an extinction peak centered at 680 nm. Individual nanocontainers were easily detectable by dark-field imaging due to their strong scattering property. This feature may allow real time imaging of the drug carrier *in vitro* and *in vivo* for pharmacokinetic and pharmacodynamic studies.[11,18] In contrast, fluorescence of the doped fluorophores was hard to image, because (1) incident light and fluorescence (centered at 517 nm) at a relatively short wavelengths transmitting in and out of nanocontainers were attenuated by the gold shell[19] and (2) at a concentration of 32 mM, the dye molecules were self-quenched significantly. Only a faint fluorescence signal was detected for closely packed nanocontainer clusters (by drying nanocontainer solution on a coverslip). Switching between dark-field and fluorescence imaging modes for the same sample shows virtually complete overlap of the scattering and fluorescence signals (Figure 2c and d), suggesting that the dye molecules are indeed trapped inside the nanocontainers. We further tested the technology with a common anticancer drug, Doxorubicin, which is also a fluorescent molecule. Similar results were obtained as shown in Figure 2e−h, indicating this technology could become a general approach for encapsulating various therapeutic compounds or a cocktail of them. The fluorescence image shows a much improved contrast than that of the doped FAM because of doxorubicin's favorable spectral properties, in particular the longer emission wavelength (less transmission attenuation[19]) and the larger fluorescence Stokes shift, both of which help reduce background autofluorescence.

Because FAM is efficiently quenched inside the gold nanocontainer, its fluorescence recovery after release can be used to monitor the stability of the nanocontainers. Based on the current configu-

10.1021/ja9076765

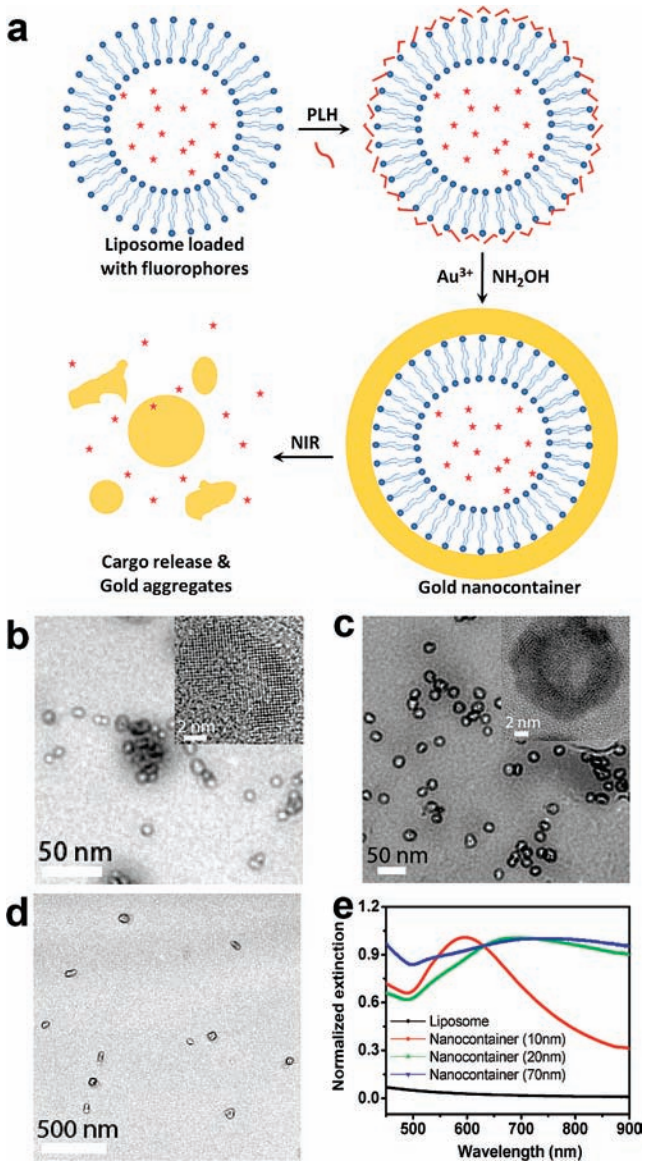

Figure 1. Nanocontainer preparation and characterization. (a) Schematic plot of gold nanocontainer (not drawn to scale) and its cargo release mechanism. Cargo (red stars) loaded liposomes are first coated with a layer of PLH for gold ion immobilization. Reduction with NH_2OH leads to formation of nanocontainers directed by the liposome scaffold. When irradiated with NIR light at their SPR, nanocontainers deform and release the contents. (b−d) TEM and HRTEM (inset) images of gold nanocontainers with mean diameters of 10 ± 3, 20 ± 5, and 70 ± 10 nm. Gold crystalline structure is seen in some small nanocontainers such as the inset image in panel b. (e) Corresponding extinction spectra of the three gold nanocontainers. Compared with that of the original liposomes, the intensities of the three extinction peaks centered at ~600, 690, and 750 nm are dramatically enhanced.

ration, leakage can be easily assessed if FAM diffuses out, because dilution of the initially concentrated dye molecules and removal of the gold thin shell will restore its fluorescence. As shown in Figure 3a, without laser irradiation, FAM in the parent liposomes and PLH-coated liposomes quickly leached out, indicated by the increasing fluorescence intensities, reaching their maxima in 4−5 days. Slightly decreased fluorescence intensities were also seen after extended storage, likely due to photobleaching since organic dyes are not photostable. In contrast, no detectable changes of fluorescence were observed for FAM in the gold nanocontainers after several weeks of storage.

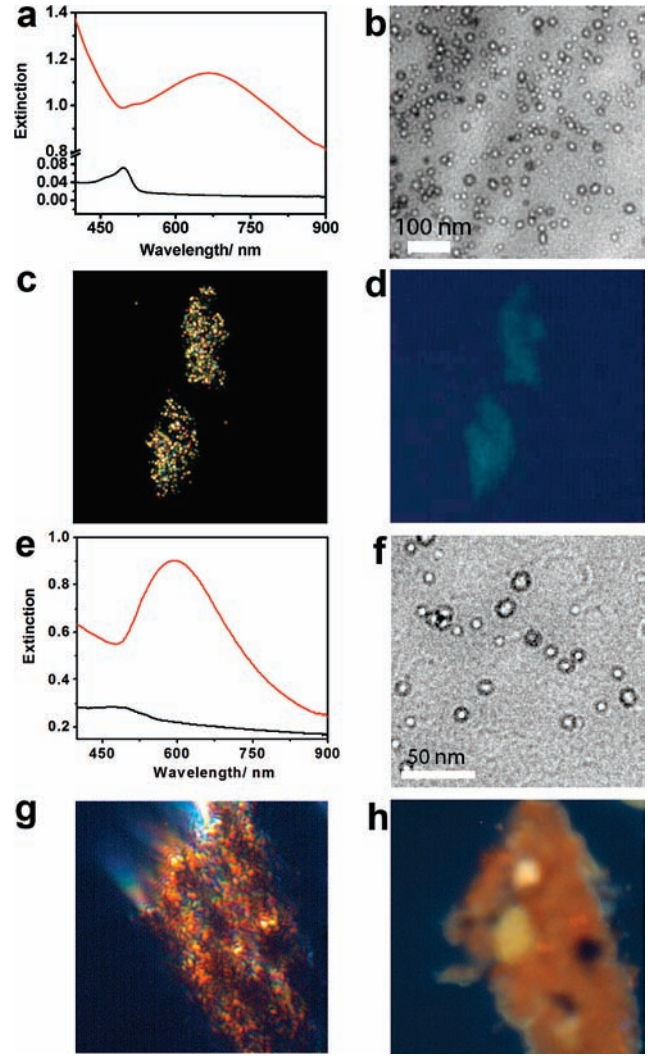

Figure 2. Gold nanocontainers loaded with FAM (a−d) and doxorubicin (e−h). (a) Extinction spectra of FAM-liposomes before and after gold shell formation. Without thin gold shells, the extinction profile is caused by FAM absorption centered at 495 nm (black). After gold nanocontainer formation, the extinction is dominated by the gold SPR band centered at ~680 nm (red). (b) TEM image of gold nanocontainers encapsulated with FAM. (c and d) Dark-field and fluorescence imaging of FAM-loaded gold nanocontainers. The nanoparticles are detectable by dark-field imaging due to the scattering property of the thin gold shell. The fluorescence signal is weak but collectively can be detected as in the case of clusters. Nanocontainers in the two images show nearly complete overlap. (e−h) Same set of experiments performed with anticancer drug, doxorubicin.

Next, we proceeded to investigate the nanocontainers' capability of releasing doped molecules mediated by NIR light illumination. As aforementioned, quick drug release responding to external stimuli is equally important as stable drug encapsulation, so that a desirable dose can be released when the carriers reach targeted disease sites. In the presence of a pulsed laser (wavelength matching nanocontainer's SPR), the release profile of FAM measured by its fluorescence shows a laser power-dependent behavior (Figure 3b). Under low energy laser irradiation such as 1.3 mJ/cm^2, FAM fluorescence increase is negligible. As the laser fluence increases (e.g., 10−20 mJ/cm^2), pronounced cargo release is revealed by the increasing fluorescence. To bring the laser power into context with human exposure safety, it is important to make sure it is below the so-called maximum permissible exposure or MPE, which is defined as the level of radiation a person receives without hazardous effects. MPE is wavelength dependent, and by the definition of American National Standard Institute (Z136.1−2000), the value is 20 mJ/cm^2 between 400 and 700 nm. Thus, the laser used in the current

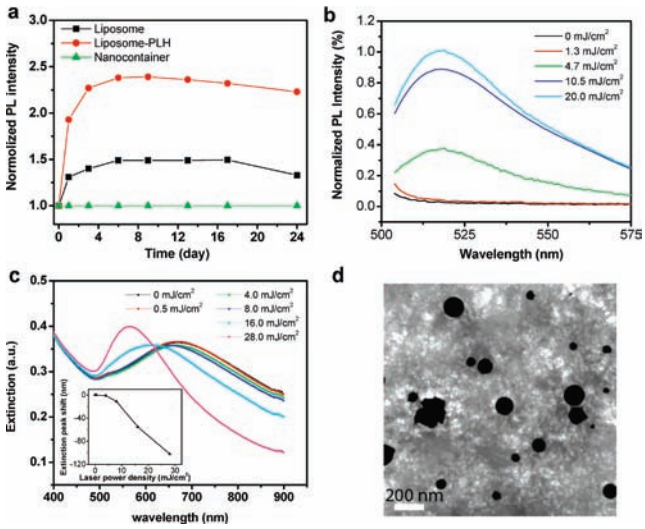

Figure 3. Stability and cargo-release capability of gold nanocontainers. (a) Dye release profiles of liposomes, PLH-coated liposomes, and gold nanocontainers, measured by the fluorescence intensity changes. The gold nanocontainers show remarkable stability with no detectable dye leakage in 24 days. (b) Cargo release triggered by pulsed laser irradiation, measured by fluorescence intensity changes. In the presence of an SPR matching laser, cargo release increases with increasing laser power. (c) Nanocontainer deformation characterized by SPR spectral shift. The nanocontainers appear stable when the laser irradiation is below 4 mJ/cm^2 but deform under increasing laser power, which correlates well with the fluorescence measurements. (d) TEM image of gold nanostructures after pulsed-laser irradiation at 28 mJ/cm^2, the highest laser fluence used in the current study.

study is within this safety range. We note that, in the current study, cargo release efficiency (percentage of the original encapsulated drug that is released) is not obtained. This is largely due to the difficulty in measuring the molar concentration of the gold nanocontainers. Unlike gold nanoparticles, whose size-dependent molar extinction coefficients (ε) are well established, additional systematic work is needed to determine the ε for this new type of hollow nanoparticles so that a concentration working curve can be established.

To confirm the cargo release is indeed due to gold shell deformation, two additional independent experiments were conducted. First, we measured the nanocontainer's extinction profiles after laser irradiation at various laser fluences because the SPR peaks of plasmonic nanomaterials are highly sensitive to changes in their size, shape, and local environment. As shown in Figure 3c, the SPR peak blue-shifted significantly as the laser power increased, which could potentially serve as a functional assay to monitor drug release because loaded drugs are not necessarily fluorescent unlike the current model system. It has been recently pointed out by Gambhir and co-workers that, in drug delivery applications, the physical location of the drug or drug carrier is not the only parameter that is useful to monitor; the release of the drug to disease sites and the biological response are also of strong interest for effective therapeutics.[20] The other independent measurement was based on TEM, as shown in Figure 3d. After laser illumination, the majority of the nanocontainers are converted to large gold aggregates, which unambiguously demonstrates the deformation of nanocontainer. Although bulk gold has a melting temperature above 1000 °C, it has been known for decades that nanoparticle gold melts at a much lower temperature depending on size.[21] Judging from the sizes of the gold nanoparticles after NIR light illumination and the original nanocontainers, it is clear that multiple nanocontainers must have aggregated together. Likely the thiolated PEG dissociates from the gold surface, leading to aggregation of the deformed nanocontainers. Similarly, this kind of light-induced aggregation or fusion phenomenon has been observed previously on other plasmonic nanomaterials, such as gold nanocages and nanorods.[22,23] Systematic study on the dissociation of thiolated molecules from a gold surface has also been reported previously. It was suggested that the gold−sulfur bond breaking is one of the pathways for nonradiative relaxation of optically excited electrons within gold nanoparticles.[24] Without the PEG protection layer, colloidal particles are prone to aggregation.

In summary, we have developed a new technology based on gold nanocontainers for spatially and temporally controlled drug delivery. As a proof of concept, a nanocontainer was doped with model cargo molecules, organic dye FAM, and anticancer drug doxorubicin, which could also be efficiently released triggered by NIR laser irradiation. In comparison with traditional plasmonics-based technologies where drugs are either immobilized on nanoparticle surfaces or embedded inside liposomes decorated with gold nanoparticles, this new generation of drug carrier is leakage-free over extended storage, monodisperse and compact in size, spectrally programmable by varying the particle size and shell thickness, responsive to light irradiation, and offers an important mechanism for monitoring drug release profiles. These features could open exciting opportunities in nanosciences, controlled and traceable drug delivery, molecular imaging, and fundamental biophysics.

Acknowledgment. This work was supported in part by grants to X.H.G. from the NIH (R01 CA131797, R01 CA140295), NSF (0645080), and University of Washington. X.H.G. thanks the NSF for a Faculty Early Career Development award (CAREER). We are especially grateful to Prof. Matt O'Donnell, Dr. Shengwen Huang, and Dr. Congxian Jia for help with the laser irradiation experiments.

Supporting Information Available: Detailed experimental procedure. This information is available free of charge via the Internet at http://pubs.acs.org.

References

(1) Zhao, W. A.; Karp, J. M. *Nat. Mater.* **2009**, *8*, 453–454.
(2) Jones, M. R.; Millstone, J. E.; Giljohann, D. A.; Seferos, D. S.; Young, K. L.; Mirkin, C. A. *ChemPhysChem* **2009**, *10*, 1461–1465.
(3) Lee, S. E.; Liu, G. L.; Kim, F.; Lee, L. P. *Nano Lett.* **2009**, *9*, 562–570.
(4) Braun, G. B.; Pallaoro, A.; Wu, G. H.; Missirlis, D.; Zasadzinski, J. A.; Tirrell, M.; Reich, N. O. *ACS Nano* **2009**, *3*, 2007–2015.
(5) Volodkin, D. V.; Skirtach, A. G.; Mohwald, H. *Angew. Chem., Int. Ed.* **2009**, *48*, 1807–1809.
(6) Troutman, T. S.; Leung, S. J.; Romanowski, M. *Adv. Mater.* **2009**, *21*, 2334–2338.
(7) Chen, C. C.; Lin, Y. P.; Wang, C. W.; Tzeng, H. C.; Wu, C. H.; Chen, Y. C.; Chen, C. P.; Chen, L. C.; Wu, Y. C. *J. Am. Chem. Soc.* **2006**, *128*, 3709–3715.
(8) Takahashi, H.; Niidome, Y.; Yamada, S. *Chem. Commun.* **2005**, 2247–2249.
(9) Wu, G. H.; Milkhailovsky, A.; Khant, H. A.; Fu, C.; Chiu, W.; Zasadzinski, J. A. *J. Am. Chem. Soc.* **2008**, *130*, 8175–8177.
(10) Jain, T. K.; Morales, M. A.; Sahoo, S. K.; Leslie-Pelecky, D. L.; Labhasetwar, V. *Mol. Pharmacol.* **2005**, *2*, 194–205.
(11) Qi, L.; Gao, X. *ACS Nano* **2008**, *2*, 1403–1410.
(12) Torchilin, V. P. *Nat. Rev. Drug Discov.* **2005**, *4*, 145–160.
(13) Chen, H.; Kim, S.; He, W.; Wang, H.; Low, P. S.; Park, K.; Cheng, J.-X. *Langmuir* **2008**, *24*, 5213–5217.
(14) Chen, H. T.; Kim, S. W.; Li, L.; Wang, S. Y.; Park, K.; Cheng, J. X. *Proc. Natl. Acad. Sci. U.S.A.* **2008**, *105*, 6596–6601.
(15) Jin, Y. D.; Gao, X. H. *Nat. Nanotechnol.* **2009**, *4*, 571–576.
(16) Kalambur, V. S.; Longmire, E. K.; Bischof, J. C. *Langmuir* **2007**, *23*, 12329–12336.
(17) Volkov, A. N.; Sevilla, C.; Zhigilei, L. V. *Appl. Surf. Sci.* **2007**, *253*, 6394–6399.
(18) Medarova, Z.; Pham, W.; Farrar, C.; Petkova, V.; Moore, A. *Nat. Med.* **2007**, *13*, 372–377.
(19) Liao, S. Y. *IEEE Trans. Electromag. Compat.* **1975**, *-17*, 211–216.
(20) de la Zerda, A.; Gambhir, S. S. *Nat. Nanotechnol.* **2007**, *2*, 745–746.
(21) Buffat, P.; Borel, J. P. *Phys. Rev. A* **1976**, *13*, 2287–2298.
(22) Hu, M.; Petrova, H.; Chen, J. Y.; McLellan, J. M.; Siekkinen, A. R.; Marquez, M.; Li, X. D.; Xia, Y. N.; Hartland, G. V. *J. Phys. Chem. B* **2006**, *110*, 1520–1524.
(23) Link, S.; Wang, Z. L.; El-Sayed, M. A. *J. Phys. Chem. B* **2000**, *104*, 7867–7870.
(24) Jain, P. K.; Qian, W.; El-Sayed, M. A. *J. Am. Chem. Soc.* **2006**, *128*, 2426–2433.

JA9076765